An analytical model for vibrational non-Born–Oppenheimer induced electron ejection in molecular anions

Jack Simons
Chemistry Department and Henry Eyring Center for Theoretical Chemistry, University of Utah, Salt Lake City, Utah 84112

(Received 8 July 2002; accepted 29 August 2002)

We introduce an analytical model designed to capture the most important features of the electronic matrix elements arising in non-Born–Oppenheimer couplings between a bound anion state and a neutral-molecule-plus-ejected-electron state. In this particle-in-a-radial-box model, vibrations are assumed to cause modulations in the depth (U^0) and length (L) parameters of the box. The most important elements of this model are that L is chosen to reproduce the proper dependence of the radial size of the anion's orbital on electron binding energy, and U^0 is chosen to produce the correct electron affinity. Within this model, which is shown to be consistent with trends seen in *ab initio* calculations of associated electron ejection rates, the coupling matrix elements can be evaluated analytically to provide closed-form expressions for how the rates depend upon (1) the kinetic energy of the ejected electron, (2) the energy spacing between the anion and neutral energy surfaces as a function of geometry, (3) the difference in the slopes of the anion and neutral energy surfaces, and (4) overlaps of the neutral's vibration–rotation wave function with the spatial derivative of that of the anion. © *2002 American Institute of Physics.* [DOI: 10.1063/1.1515766]

I. INTRODUCTION

For nearly 30 years, our research group has been involved in theoretical studies of molecular anions.[1] As a part of these studies, the mechanism by which excess vibrational energy can be converted into electronic energy to cause electron ejection to produce an unbound electron and a neutral molecule has been the subject of considerable study.[2–7] *Ab initio* electronic structure calculations have allowed us to gain considerable insight into these detachment processes. However, until now, we did not possess a simple physical picture in terms of which to understand, in a semiquantiative manner, many results of our simulations. It is the primary focus of the present effort to produce a physical model that provides such insight. In particular, this work deals with the electronic non-Born–Oppenheimer (non-BO) matrix elements that enter into the expression for the electron ejection rates and produces a closed analytical expression for how these rates depend upon the essential physical parameters of the anion and neutral.

A. Nature of the non-BO processes

Before describing the model we have developed, it is important to clarify the physical origins of the phenomena that this model is designed to address. To explain what is not involved in the radiationless transitions we study, let us compare these events to what happens when an electronically excited molecule emits a photon (see Fig. 1).

The electron ejection event illustrated here is very different from photon emission. In the latter, a photon comes out and the molecule evolves to a state of lower total and lower electronic energy. In the former, an electron comes out and the system evolves to a state of lower total energy but to a state of higher electronic energy. So, in photon emission, the final state has lower electronic energy; in the electron ejection events of interest here, the final state has the higher electronic energy.

B. Perturbative treatment of non-BO rates

What causes the molecule to be able to move to a state of higher electronic energy is the coupling between the electronic and nuclear-motion (i.e., vibrational and rotational) energies. These non-Born–Oppenheimer (non-BO) couplings provide a means for excess vibrational energy to be converted into electronic energy, which then leads to an electron being ejected. We showed long ago[2,8] that, within a perturbative regime where the non-BO couplings are weak and thus the rate of electron ejection slow, the rates R (in ejections per second) at which these processes can eject electrons can be written as follows:

$$R=(2\pi/\hbar)\int |\langle\chi_i|\langle\psi_i|P|\psi_f\rangle(P/\mu)\chi_f\rangle|^2 \times\delta(\varepsilon_f+E-\varepsilon_i)\rho(E)dE. \quad (1)$$

Here, χ_i and χ_f are the vibration–rotation wave functions of the anion and neutral, respectively, ψ_i is the electronic wave function of the anion, ψ_f is that of the neutral-plus-ejected electron, and $\rho(E)$ is the density of translational states of the electron ejected with kinetic energy E. The $\delta(\varepsilon_f+E-\varepsilon_i)$ quantity guarantees that the total energy of the initial state ε_i matches that of the final state ε_f plus the ejected electron E. The momentum operators (P) appearing above act on both the electronic and vibration–rotation functions as follows:

$$(P\psi_f)(P/\mu)\chi_f=\Sigma_a(-i\hbar\nabla_a\psi_f)(-i\hbar\nabla_a\chi_f)(1/m_a). \quad (2)$$

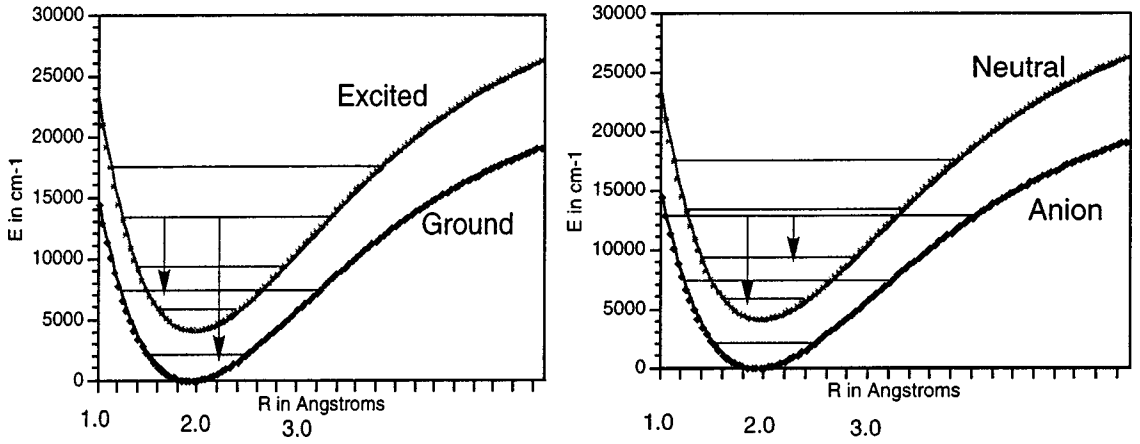

FIG. 1. Ejection of photons from an electronically excited molecule in a specific vibrational level to two different vibrational levels of the ground electronic state (left-hand side). Ejection of an electron from an excited vibrational level of an electronically stable anion to a less excited vibrational level of the neutral (right-hand side).

This expression involves a sum over all of the nuclei (labeled a) of derivatives (∇_a) with respect to the positions of the nuclei, as well as the masses of the nuclei (m_a); the notation P/μ is used to remind one that there are $1/m_a$ factors in the operator.

The above rate expression contains two kinds of matrix elements: (1) those that involve integration over the electrons' coordinates (they form the focus of the present work)

$$m_{i,f}=\langle \psi_i|(-i\hbar\nabla_a)|\psi_f\rangle \tag{3}$$

and (2) vibration–rotation integrals (that we have treated in earlier works[7,9–11])

$$\langle \chi_i|m_{i,f}(-i\hbar\nabla_a\chi_f)\rangle. \tag{4}$$

In the latter, the electronic non-BO integral appears inside the integral because the quantity $m_{i,f}$ is a function of the internal coordinates (i.e., bond lengths, angles, and orientation) of the anion.

C. Contrasts with the photon absorption rate expression

The rate expression for photon absorption connecting initial electronic ψ_i and vibration–rotation χ_i states to final states ψ_f and χ_f involves analogous integrals. In particular, the electric dipole integral

$$\mu_{i,f}=\langle \psi_i|\mu|\psi_f\rangle \tag{5}$$

and the vibrational integral

$$\langle \chi_i|\mu_{i,f}\chi_f\rangle \tag{6}$$

appear in such expressions. In the optical spectroscopy case, one often expands the geometry dependence of $\mu_{i,f}$ about the equilibrium geometry of the ground state:

$$\mu_{i,f}=\mu^0_{i,f}+\Sigma_a(\partial\mu_{i,f}/\partial X_a)^0(X_a-X^0_a)+\dots, \tag{7}$$

where X_a denotes the Cartesian coordinates of the ath atom, and X^0_a denotes its equilibrium value. Inserting this expansion into the $\langle \chi_i|\mu_{i,f}\chi_f\rangle$ integral and retaining only the lead term ($\mu^0_{i,f}$) reduces the vibrational integral to those occurring in the well known Franck–Condon factors:

$$\langle \chi_i|\mu_{i,f}\chi_f\rangle=\mu^0_{i,f}\langle \chi_i|\chi_f\rangle. \tag{8}$$

The intensities of photon absorption lines are thus related to squares of the $\mu^0_{i,f}$ electronic matrix elements and of the vibrational overlap integrals $\langle \chi_i|\chi_f\rangle$.

The treatment outlined above is predicated on the assumptions that

(1) the electronic transition moment $\mu_{i,f}$ has a significant value at the equilibrium geometry where χ_i also is most significant, and
(2) this moment $\mu_{i,f}$ is rather slowly varying for geometries somewhat displaced from the equilibrium geometry $\{X^0_a\}$, which is why the Taylor expansion in Eq. (7) is used.

Our experience[2–6] has shown us that the analogs of these two assumptions are not usually valid when dealing with non-BO matrix elements. In particular, the electronic integral $m_{i,f}$ cannot be assumed to be significant at geometries where the initial vibrational wave function has large amplitude. Instead, the results of our many *ab initio* calculations of such matrix elements convinced us that $m_{i,f}$ is largest when the anion and neutral electronic energy surfaces are closest. Moreover, it has not been found in the *ab initio* calculations we have performed that $m_{i,f}$ varies weakly with geometrical displacements. Instead, as the geometry moves away from where the anion and neutral surfaces are closest, $m_{i,f}$ decreases rapidly. We illustrate this kind of behavior in Fig. 2.

Based on a substantial number of *ab initio* calculations,[2–6] we have concluded that contributions to the rate expression given in Eq. (1) are large whenever

(1) the anion and neutral electronic energy surfaces are close in energy, and
(2) the phases and local de Broglie wavelengths $\lambda_{i,f}$ of χ_i and of $d\chi_f/dX_a$ are similar at the same geometries where $m_{i,f}$ is large.

The first condition appears to be what causes $m_{i,f}$ to be large, as we address in further detail later and as our analyti-

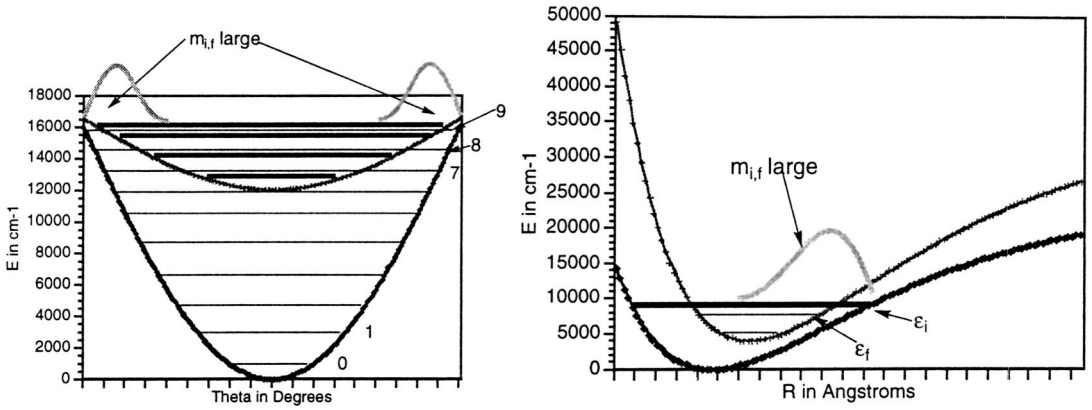

FIG. 2. Two examples of anion (lower) and neutral (upper) surfaces that approach closely showing where $m_{i,f}$ is largest and how $m_{i,f}$ varies with geometry.

cal model correctly reproduces. The second condition is what causes contributions to the integral involving the product of $m_{i,f}$, χ_i, and $d\chi_f/dX_a$ to be significant. That $d\chi_f/dX_a$ and not χ_f appears in the rate expression relates to the fact that momentum as well as energy is transferred in the radiationless transition; so, the momentum operators $(-i\hbar\nabla_a)$ must act on χ_f to couple it to χ_i. Within the harmonic approximation, the derivatives $d\chi_f/dX_a$ produce vibrational wave functions having one higher and one lower quantum number; it is the latter that contributes to the integral and allows one unit of vibrational momentum to be converted to electronic momentum [as reflected in the fact that $m_{i,f}=\langle\psi_i|(-i\hbar\nabla_a)|\psi_f\rangle$ also contains a momentum transition element].

D. Focus of the present work

Most of our past works in this area have been directed toward either (1) using *ab initio* electronic structure methods to calculate, via. Eq. (1), non-BO induced electron ejection rates for specific anions of experimental interest, or (2) analyzing[2,7,9–11] the vibrational or rotational components of the $\langle\chi_i|m_{i,f}(-i\hbar\nabla_a\chi_\phi)\rangle$ matrix elements that govern the rate to arrive at propensity rules with respect to angular momentum and vibrational energy and momentum changes.

In the present paper, our efforts are focused on obtaining further insight into the electronic matrix elements $m_{i,f}$ by introducing an approximate yet reasonable model that allows us to derive analytical expressions for how these matrix elements depend on (a) the energy gap between the anion and neutral potential energy surfaces, and (b) the kinetic energy carried away by the ejected electron. It is these analytical expressions and the model used to achieve them that represent the primary results of this work.

II. ANALYSIS OF THE ELECTRONIC NON-BO ELEMENTS

A. Physical meaning of the non-BO elements

The electronic integrals $m_{i,f}=\langle\psi_i|(-i\hbar\nabla_a|\psi_f\rangle$ can be expressed in terms of the overlap of either the initial (anion) or final (neutral-plus-free-electron) wave function with the derivative of the other wave function. That is, because the two functions are orthogonal for all values of the nuclear positions [denoted (X_a)],

$$\langle\psi_i|\psi_f\rangle=0, \tag{9}$$

the following identity holds for derivatives with respect to any nuclear position:

$$\langle\psi_i|d/dX_a|\psi_f\rangle=-\langle\psi_f|d/dX_a|\psi_i\rangle. \tag{10}$$

So, in computing the non-BO electronic matrix elements $m_{i,f}$ we can differentiate either the anion or the neutral plus free electron wave function.

The most general form for the anion wave function ψ is the linear combination of determinants form

$$\psi=\sum_J C_J|\phi_{J1}\,\phi_{J2}\cdots\phi_{JN}|, \tag{11}$$

where the C_J are the so-called configuration interaction coefficients, ϕ_{Jk} is the spin–orbital occupied by the kth electron, and the $|\cdots|$ notation denotes the determinant formed from the product of N such spin–orbitals. In turn, each of the molecular spin–orbitals (MO) is written as a linear combination of atomic orbital (AO) basis functions $\{\eta_\mu\}$ multiplied by a linear combination of atomic orbital to form molecular orbital (LCAO–MO) coefficients $C_{k,\mu}$.

The derivative of such a wave function with respect to any internal vibrational distortion of the molecule, which we denote d/dX, will involve three distinct kinds of factors:

(1) derivatives of the C_J coefficients dC_J/dX,
(2) derivatives of the $C_{k,\mu}$ coefficients $dC_{k,\mu}/dX$, and
(3) derivatives of the atomic orbital basis functions $d\eta_\mu/dX$.

The $d\eta_\mu/dX$ contributions can induce different angular character into the function, but are usually found to make small contributions to the net rate of detachment whenever the $dC_{k,\mu}/dX$ contributions are significant. For example, in Fig. 3 we show how the radial and angular derivatives, respectively, of a p_π orbital on the nitrogen center of NH^- produce d_π and p_σ character, respectively. The radial derivative arises when considering vibration-assisted electron detachment processes such as we are dealing with here. The angular derivative relates to rotational detachment events

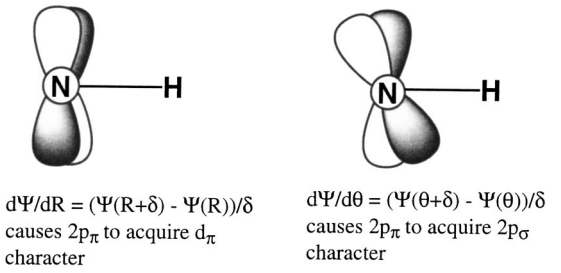

FIG. 3. Radial (left-hand side) and angular (right-hand side) derivatives of a p_π orbital on the nitrogen center of NH^-.

that do not form the focus of the present discussion (but which we and others have discussed earlier[5,7,12]).

As stated above, the $d\eta_\mu/dX$ derivatives do not usually contribute strongly to the $d\psi/dX$ factors; instead, the $dC_{k,\mu}/dX$ factors are found to dominate in most cases. Moreover, because most anions and their corresponding ground-state neutrals are described qualitatively correctly at the single-determinant level, it is common for the dC_J/dX contributions to also be small (because only one C_J is significant and thus has the fixed value of unity). For these reasons, we will focus further attention on the usually dominant, $dC_{k,\mu}/dX$ factors and their contributions to the detachment rates.

Assuming that the above $dC_{k,\mu}/dX$ are the primary derivatives in $d\psi/dX$, and making a single-determinant approximation to the anion and the neutral-plus-free-electron wave functions, the non-BO electronic integral can be reduced as follows:

$$\langle \psi_i | d/dX_a | \psi_f \rangle = \langle \phi_i | d\phi_f/dX \rangle = \Sigma_{\mu,v} C_{i,\mu}\, dC_{f,v}/dX \langle \eta_\mu | \eta_v \rangle. \quad (12)$$

The integral between the two Slater determinants reduces to an integral between the orbital ϕ_i from which the electron is ejected and the continuum orbital ϕ_f into which it is ejected. That one-electron integral, in turn, reduces to the sum of overlap integrals $\langle \eta_\mu | \eta_v \rangle$ between pairs of basis orbitals multiplied by LCAO–MO coefficients $C_{i,\mu}$ and their derivatives $dC_{f,v}/dX$. The physical meaning of an orbital derivative such as $d\phi_i/dX$ is illustrated in Fig. 4 where we show how the radial extent of an orbital changes as the bond connecting atoms near this orbital vibrate.

The molecular orbitals ϕ_i depicted above change their radial sizes by modifying their LCAO–MO coefficients $C_{k,\mu}$ in a way that causes the $C_{k,\mu}$ for more diffuse basis orbitals η_μ to grow at the expense of the $C_{k,\mu}$ for more compact basis orbitals as the $A-B$ bond shortens. The reason behind this expansion of the orbital size as the $A-B$ bond contracts lies in the fact that the anion's electron binding energy (EA) shrinks as the $A-B$ bond shortens. That is, the energy spacing between the anion and neutral energy surfaces decreases as the bond shortens.

Such variation of EA with R would, for example, occur in species such as FLi^- where the excess electron is bound in a σ orbital (such as that shown in Fig. 4) localized on the positive Li center; as the negative F atom moves closer to Li, the potential binding this electron becomes less attractive, so the EA decreases. Hence, for short $A-B$ distances, the EA is smaller, so the orbital's radial extent is large. It is this dynamical expansion and contraction (as the vibrational motion subsequently lengthens the $A-B$ bond) of the orbital that allows for vibration-to-electronic energy and momentum coupling. Another example of the variation in orbital size and binding energy is given in Fig. 5 where the orbital holding the excess electron of an enolate anion is depicted. In this example, as the twist angle evolves away from 0°, the delocalization of the p_π orbital containing the excess electron is lost making this orbital less stable, so its electron binding energy is reduced, and, in turn, its radial extent grows.

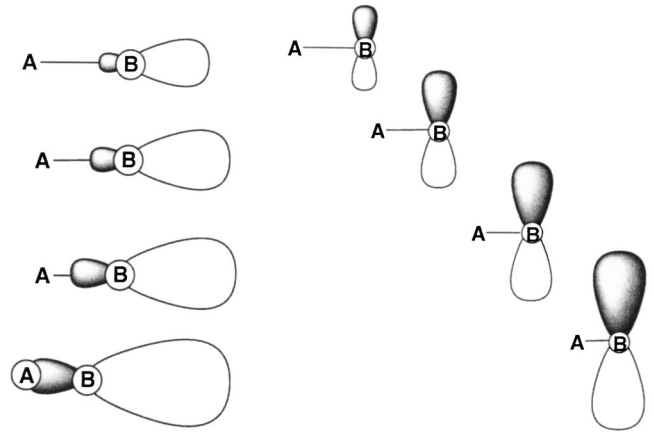

FIG. 4. Change in radial extent of an orbital induced by shortening the $A-B$ bond length for an orbital of σ (left-hand side) or of π (right-hand side) character.

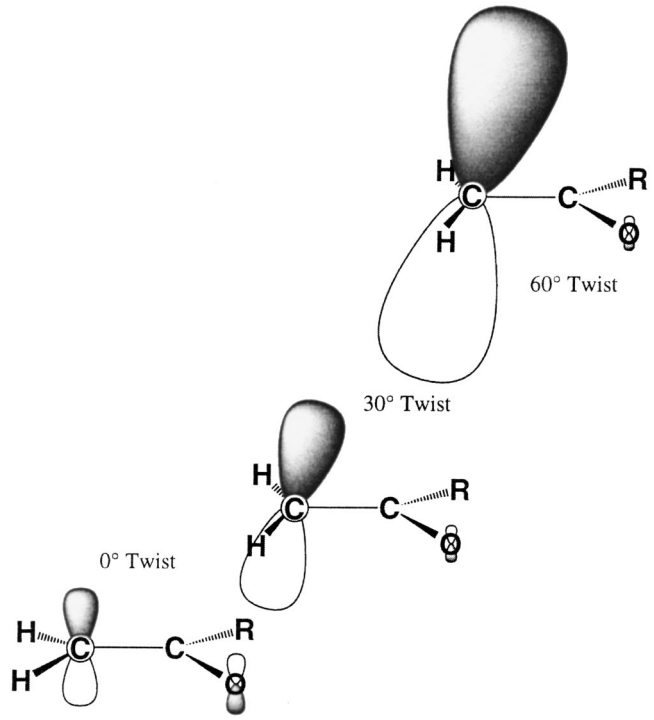

FIG. 5. Orbital holding excess electron in an enolate anion as a function of the twist angle of the terminal H_2C group.

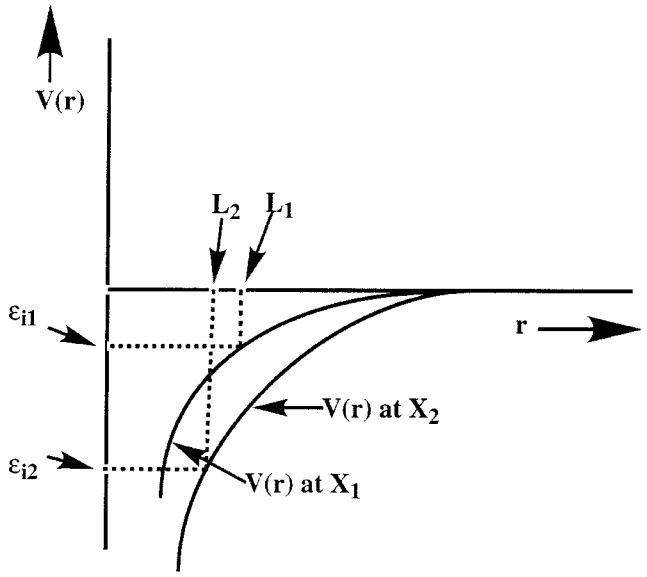

FIG. 6. Electron-molecule radial potentials $V(r)$ at two values of the vibrational coordinate X. At X_1 the potential is less attractive than at X_2.

B. An analytical model for the bound and continuum orbitals

An elementary model for describing one excess electron (whose position is given by coordinates r, θ, ϕ) interacting with a molecule (whose vibrational coordinates are denoted $\{\mathbf{X}\}$ and whose spatial orientation is described by Euler angles α, β, χ) involves a one-electron Schrödinger equation of the form

$$\{-\hbar^2/2mr^{-2}\,\partial/\partial r(r^2\partial/\partial r)+\hbar^2L^2/2mr^2+V\}\Psi=E\Psi. \tag{13}$$

In this equation, the potential V depends on the coordinates of the excess electron with respect to the molecular frame. For example, in the two cases depicted in Fig. 4, V could be of the form

$$V=-\mu e\cos\theta/2r^2 \tag{14a}$$

or

$$V=-v(r)\sin^2\theta. \tag{14b}$$

The form in Eq. (14a) could be appropriate to the σ state shown in Fig. 4 if the dominant potential were the charge-dipole potential. Here, μ is the magnitude of the dipole moment of the $A-B$ molecule, r is the distance of the electron from the positive B atom, and θ is the angular coordinate of the electron relative to the $A-B$ bond axis. Equation (14b) would apply to the π state of Fig. 6. Then, the $\sin^2\theta$ dependence shows the axially symmetric nature of the potential about the $A-B$ bond axis, and $v(r)$ would characterize how V depends on the distance (r) of the excess electron from the atom to which it is most strongly bound. In this case, $v(r)$ cannot be written in terms of a single dominant power of r as in the electron–dipole example because $v(r)$ arises from the attraction of the valence excess electron to the nucleus where its orbital is localized. However, in all cases, the radial dependence of V is attractive at large r and repulsive at small r.

An example of the former case is provided by the dipole-bound anion $FLi^-(X\,^2\Sigma^+)$ and of the latter by the valence-bound anion $HN^-(X\,^2\Pi^-)$. Of course, in the above examples, there is only one internal vibrational coordinate, the $A-B$ bond length, upon which V depends. In general, V will depend on all of the anion's vibrational coordinates, although it usually depends strongly on only one or a few (i.e., those that vibrate atoms to which the excess electron is bound) such coordinates.

To further develop our model, we now assume that

(a) the angular form of the orbital Ψ is known (e.g., it would be a σ orbital comprised primarily of s and p_σ basis orbitals for the first case shown in Fig. 4 or a π orbital comprised primarily of p_π basis orbitals in the latter), and

(b) the vibration effecting the electron ejection does not change the angular form of this orbital (e.g., the $A-B$ bond vibration shown in Fig. 4 retains the σ and π symmetries of the two orbitals shown; only the radial character of Ψ is altered).

Even in cases such as that depicted in Fig. 5 where the precise angular character of the orbital is not maintained (although that of its dominant carbon p_π nature is retained), the above two assumptions are nearly met, so the analysis offered below is assumed to still apply.

In such cases, the orbital Ψ can be expressed as a product of a fixed angular part $F(\theta,\phi)$ and a radial part $R(r)$, with the latter containing all of the vibration-coordinate $(\mathbf{X})$ dependence

$$\Psi=F(\theta,\phi)R(r|\mathbf{X}). \tag{15}$$

Such a separation of fixed angular and $\mathbf{X}$-dependent radial parts holds for both the anion orbital $(\Psi=\phi_i)$ and the continuum free-electron orbital $(\Psi=\phi_f)$,

$$\phi_i=F(\theta,\phi)R_i(r|\mathbf{X}), \tag{16a}$$

$$\phi_f=F(\theta,\phi)R_f(r|\mathbf{X}). \tag{16b}$$

When these product forms are separated into the Schrödinger equation [Eq. (13)], and one premultiplies by $F^*(\theta,\phi)\sin\theta$ and integrates over θ and ϕ, one obtains an equation for the radial parts $R_{i,f}$ of the two orbitals,

$$\{-\hbar^2/2mr^{-2}\,\partial/\partial r(r^2\,\partial/\partial r)+\hbar^2\langle L^2\rangle/2mr^2+\langle V\rangle\}R_{i,f}$$
$$=E_{i,f}R_{i,f}. \tag{17}$$

In these two radial equations, the symbol $\langle L^2\rangle$ is used to denote the average value of the angular momentum squared L^2 taken with respect to the angular "shape" of the orbitals $F(\theta,\phi)$:

$$\langle L^2\rangle=\int F^*(\theta,\phi)L^2F(\theta,\phi)\sin\theta\,d\theta\,d\phi. \tag{18}$$

The symbol $\langle V\rangle$ is used to denote the electron–molecule interaction potential V averaged over the angular coordinates with respect to this same $F(\theta,\phi)$,

$$\langle V\rangle=\int F^*(\theta,\phi)VF(\theta,\phi)\sin\theta\,d\theta\,d\phi. \tag{19}$$

By next rewriting the $R_{i,f}$ functions as

$$R_{i,f}=\psi_{i,f}/r, \tag{20}$$

Eq. (17) can be rewritten as a Schrödinger equation for the $\psi_{i,f}$ functions,

$$\{-\hbar^2/2m\,\partial^2/\partial r^2+U\}\psi_{i,f}=E_{i,f}\psi_{i,f}. \tag{21}$$

Here, we introduced the short-hand notation U to represent the sum[13] of the angularly averaged electron–molecule potential $\langle V\rangle$ and the average centrifugal potential $\hbar^2\langle L^2\rangle/2mr^2$:

$$U=\langle V\rangle+\hbar^2\langle L^2\rangle/2mr^2. \tag{22}$$

Recall that it is only through $\langle V\rangle$ that the potential in the Schrödinger equation acquires its dependence on the vibrational coordinates $\{\mathbf{X}\}$.

Now, we introduce a simple yet reasonable treatment of how U depends on $\mathbf{X}$ to further develop our model. In particular, we pose that it is the strength of the attractive electron-molecule potential $V(r)$ that is modulated as the vibration along X takes place. Typical forms for the attractive portions of such radial potentials are shown in Fig. 6 for two values (X_1 and X_2) of the vibration coordinate X. In these plots, we show the longer-range attractive portion of the potential only; of course, at smaller r values, core repulsion and exchange effects dominate and $V(r)$ becomes positive. Also shown in Fig. 6 are the ground-state anion energy levels ε_{i1} and ε_{i2} as well as the classical outer turning points L_1 and L_2 of these levels for each of the two geometries. Because the potential U is less attractive at X_1 than at X_2, the electron binding energy ε_{i1} is smaller in magnitude than ε_{i2}. In addition, the outer turning point L_1 for the less tightly bound level is larger (as is the radial extent of the corresponding orbital) than L_2. These characteristics of the potential play very important roles in how we choose the parameters of our model potential as we now illustrate.

For the model potential introduced below, we use a radial "box potential" whose outer wall (at $r=L$) and whose depth (U^0) parameters are chosen to reflect the attributes of the actual radial potential discussed above (i.e., as in Fig. 6). In particular, the depth U^0 is chosen so that the resultant lowest eigenvalue ε_i gives (through $\mathrm{EA}=U^0-\varepsilon_i$) the correct electron affinity (EA) at each particular value of X. In addition, the box length L is chosen so that the radial extent of the corresponding orbital depends on X as expected (i.e., grows as the EA decreases). Specifically, we use the fact that the true anion orbital varies as $r\exp(-r(2m\,\mathrm{EA}/\hbar^2)^{1/2})$ for large r, which suggests that the average value of r should depend on EA as follows:

$$\langle r\rangle=3\hbar/(2(2m\,\mathrm{EA})^{1/2})=(3/2^{3/2})(\hbar/m^{1/2})\mathrm{EA}^{-1/2}. \tag{23}$$

Below, we use this relationship between $\langle r\rangle$ and EA to relate the radial potential's box length parameter L to EA.

It is important to stress that our primary goal in this work is not to accurately calculate (i.e., obtain a numerical value for) the $m_{i,f}$ non-BO matrix elements; we already know how to do this using *ab initio* quantum chemistry. Instead, our objective is to obtain analytical expressions for how $m_{i,f}$ depends on the EA (as a function of geometry) and on the kinetic energy E carried away by the ejected electron. To this end, we introduce a rather simple, but we believe qualitatively correct, model for the effective potential and for how this potential depends on the vibrational coordinates $\mathbf{X}$. Within this model, we are then able to analytically evaluate $m_{i,f}$ in a way that allows us to display its EA and E dependencies. Because this model is qualitatively representative of actual electron-molecule interactions, we thus believe that its E and EA dependencies are suggestive of what is found in reality.

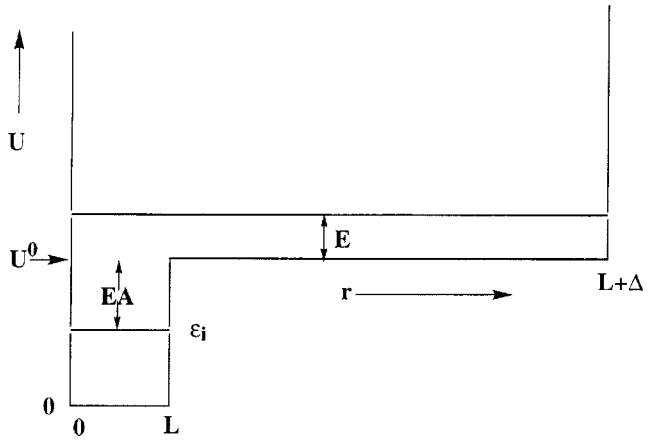

FIG. 7. Radial effective potential $U(r)$ showing bound-state energy ε_i, continuum-state kinetic energy E, well depth U^0, and potential radial extent L.

Proceeding with the development of our model, the effective radial potential $U(r)$ is represented by a square-well box potential such as shown in Fig. 7. The energy difference between the well depth U^0 and the bound-state energy ε_i is the electron affinity EA ($\mathbf{X}$). The dependence of this EA on the vibrational coordinates $\{\mathbf{X}\}$ is assumed to arise totally from modulations in the well depth U^0 and L parameters. In particular, we use the relation that $U^0=\mathrm{EA}+\varepsilon_i$ and we assume that ε_i is given in terms of the particle in a box ground-state energy expression (see below for justification)

$$\varepsilon_i=\hbar^2\pi^2/(2mL^2). \tag{24}$$

Next, since the average value of the radial coordinate $\langle r\rangle$ for the corresponding ground-state wave function is

$$\langle r\rangle=L/2 \tag{25}$$

we use Eqs. (23) and (25) to relate the box length L to the EA as follows:

$$L=2\langle r\rangle=(3/2^{1/2})(\hbar/m^{1/2})\mathrm{EA}^{-1/2}. \tag{26}$$

Using this value for L in Eq. (24) allows ε_i and U^0 to be rewritten in terms of EA,

$$\varepsilon_i=\pi^2\,\mathrm{EA}/9, \tag{27a}$$

$$U^0=\mathrm{EA}(1+\pi^2/9), \tag{27b}$$

and, of course, Eq. (26) gives L in terms of EA.

As noted above, the radial extent of the bound-state anion orbital $\langle r\rangle$ is related to the outer turning point (i.e., the box length parameter L). On the other hand, the free-electron

orbital, whose asymptotic (kinetic) energy is E, is assumed to be "box normalized" to unity over the range $0 \leq r \leq L + \Delta$.

The normalized bound-state radial wave function $\psi_i(r)$ will be assumed to vanish at $r = L$ to keep the analysis as simple as possible while remaining qualitatively correct. In principal, this function should also contain an exponentially decaying component in the $r > L + \Delta$ region, but this component will be neglected. The resultant normalized ground-state anion wave function is

$$\psi_i(r) = (2/L)^{1/2} \sin(\pi r/L) \tag{28}$$

and the corresponding energy is as given in Eqs. (24) and (27a).

The free-electron solution to the radial Schrödinger equation is expressed as follows:

$$\psi_f(r) = C \sin(p^+ r/\hbar), \quad \text{for } 0 \leq r \leq L, \tag{29a}$$

$$\psi_f(r) = D \exp(ip(r-L)/\hbar) + D' \exp(-ip(r-L)/\hbar), \quad \text{for } L \leq r \leq L + \Delta. \tag{29b}$$

Here, $p = (2mE)^{1/2}$ and $p^+ = (2m(U^0 + E))^{1/2}$ are the momenta of the electron in the asymptotic region $L \leq r \leq L + \Delta$ and in the region where $U(r)$ is nonzero $r \leq L$, respectively. Matching ψ_f and $d\psi_f/dr$ at $r = L$ and normalizing ψ_f such that the integral of $|\psi|^2$ between $r = 0$ and $r = L + \Delta$ is unity

$$\int |\psi_f(r)|^2 \, dr = 1 \tag{30}$$

produces (in the $\Delta \to \infty$ limit) equations for the amplitudes C, D, and D'. These results are

$$C = (2/\Delta)^{1/2} \{\sin^2(p^+ L/\hbar) + (p^+/p)^2 \cos^2(p^+ L/\hbar)\}^{-1/2}, \tag{31a}$$

$$D = 1/2[\sin(p^+ L/\hbar) - i(p^+/p)\cos(p^+ L/\hbar)]C, \tag{31b}$$

$$D' = 1/2[\sin(p^+ L/\hbar) + i(p^+/p)\cos(p^+ L/\hbar)]C. \tag{31c}$$

Notice that all three amplitudes scale as $(1/\Delta)^{1/2}$ as expected for a box-normalized function.

C. Non-BO matrix elements

The non-BO electronic matrix element $m_{i,f}$ connecting ψ_i and ψ_f can, within the above approximations to the wave functions, be written as

$$m_{i,f} = -i\hbar \int (2/L)^{1/2} \sin(\pi r/L) \, d/dX \, C \sin(p^+ r/\hbar) dr, \tag{32}$$

where C is given in Eq. (31a) and the integral ranges over $0 \leq r \leq L$, and the derivative d/dX is meant to denote a sum of derivatives with respect to all vibrational coordinates. Changes in these coordinates are, as discussed earlier, assumed to modulate the depth of the attractive electron-molecule potential U^0 and thus the EA, which is $U^0 - \varepsilon_i$. We re-express the derivative d/dX $(C \sin(p^+ r/\hbar))$ as follows:

$$d/dX(C \sin(p^+ r/\hbar)) = (dC/dX)\sin(p^+ r/\hbar) + C(r/\hbar) dp^+/dX \cos(p^+ r/\hbar). \tag{33}$$

The first term, dC/dX, does not contribute to $m_{i,f}$ as the integral $\int \sin(\pi r/L)\sin(p^+ r/\hbar) dr$ vanishes because the bound and continuum orbitals are orthogonal to one another. The dp^+/dX factor in the second term is rewritten as

$$dp^+/dX = 1/2(2m)^{1/2}[dU^0/dX]\{U^0 + E\}^{-1/2}. \tag{34}$$

The result is that the non-BO matrix element becomes

$$m_{i,f} = -i\hbar(2/L)^{1/2} C (2m)^{1/2} (1/2\hbar)[dU^0/dX] \times \{U^0 + E\}^{-1/2} \int \sin(\pi r/L) r \cos(p^+ r/\hbar) dr. \tag{35}$$

The integral involving the trigonometric functions can be carried out and yields

$$m_{i,f} = -i\hbar^2 \pi/2(2/L)^{1/2} C[dU^0/dX] \times \{2m(U^0 + E)\}^{-1/2} \{U^0 + E - \varepsilon_i\}^{-1}. \tag{36}$$

Inserting the expression for C given in Eq. (31a), again identifying the momenta $p = (2mE)^{1/2}$ and $p^+ = (2m(U^0 + E))^{1/2}$, and recalling that $U^0 = \mathrm{EA}(1 + \pi^2/9)$ gives

$$m_{i,f} = -i\hbar^2 \pi (L\Delta)^{-1/2} \, d\,\mathrm{EA}/dX(1 + \pi^2/9)[\mathrm{EA} + E]^{-1} \times (p/p^+)\{p^2 \sin^2(p^+ L/\hbar) + p^{+2} \cos^2(p^+ L/\hbar)\}^{-1/2}. \tag{37}$$

Again, we stress that the rate of change of the EA along the vibrational coordinate X is assumed to result from the modulation in the well depth U^0 and L parameters accompanying this vibration; this is what allows us to replace dU^0/dX by $(1 + \pi^2/9) d\,\mathrm{EA}/dX$. Equation (37) represents our final result for the non-BO electronic matrix elements [keeping in mind that $L = 3\hbar/(2m\,\mathrm{EA})^{1/2}$].

D. The electron ejection rate expression

To obtain an expression for the rate of electron ejection induced by vibrational non-BO coupling, we insert Eq. (37) into Eq. (1). This produces the following rate expression (here μ is the mass factor associated with the vibrational coordinate X):

$$R = (2\pi^2\hbar^4/3\mu^2)(1 + \pi^2/9)^2 \int \left| \int \chi_i^* \, d\,\mathrm{EA}/dX \times [\mathrm{EA} + E]^{-1} (p/p^+)(2m\,\mathrm{EA}/\hbar^2)^{1/4} \{p^2 \sin^2(p^+ L/\hbar) + p^{+2} \cos^2(p^+ L/\hbar)\}^{-1/2} d\chi_f/dX \, \mathbf{dX} \right|^2 dp$$

$$= (2\pi^2\hbar^3/3\mu^2)(1 + \pi^2/9)^2 \int \left| \int \chi_i^* \, d\,\mathrm{EA}/dX \times [\mathrm{EA} + E]^{-1} [E/(E + U^0)]^{1/2} \mathrm{EA}^{1/4} (2m)^{-1/4} \{E + U^0 \cos^2[(E + U^0)/\mathrm{EA}]\}^{-1/2} d\chi_f/dX \, \mathbf{dX} \right|^2 dp, \tag{38}$$

where we have also substituted the density of states $\rho(E)dE = (\Delta/\pi\hbar) \, dp$ and the expression for $L = 3\hbar/(2m\,\mathrm{EA})^{1/2}$. The key ingredients in this rate expression that we wish to emphasize are

(1) The energy gap $(\varepsilon_i - \varepsilon_f)$ between the anion's state χ_i and the neutral's χ_f determines the kinetic energy E carried away by the ejected electron.
(2) As expected, we obtain a rate that is proportional to the square of an integral connecting the anion's vibration-rotation wave function χ_i to the derivative of the neutral molecule's corresponding wave function $d\chi_f/dX$.
(3) In this integral, a factor $d\,\mathrm{EA}/dX[\mathrm{EA}+E]^{-1}$ appears that is large when the anion and neutral energy surfaces are close (i.e., EA is small) and when the "gap" between these surfaces is changing rapidly (i.e., $d\,\mathrm{EA}/dX$ is large). This is one of the most important quantitative suggestions of this model, and is what helps us identify the geometries near where $m_{i,f}$ is large as in Fig. 2. Moreover, it is this factor that seems to fit what we have observed in all of our *ab initio* calculations when we searched for geometries where $m_{i,f}$ is largest.
(4) Also within this integral, the factor $[E/(E+U^0)]^{1/2}$ appears. This factor disfavors E values near zero, and is a rather slowly varying function of E at higher E values. Recalling that $U^0=(1+\pi^2/9)\mathrm{EA}$, this factor also disfavors geometries where EA is large.
(5) The quantity $\{E+U^0\cos^2[(E+U^0)/\mathrm{EA}]\}^{-1/2}$, which also occurs within this integral, is limited in magnitude between (i) $E^{-1/2}$ and (ii) $(U^0)^{-1/2}$. This is also a rather weak function of E and of U^0 (which is proportional to EA).

III. SUMMARY

We have introduced a one-dimensional particle-in-a-radial-box model for the electron-molecule potential of a molecular anion. In this model, the vibrations of the underlying nuclear framework are assumed to cause modulations in the depth (U^0) and length (L) of the attractive potential well. These modulations, in turn, induce dynamical changes in the radial size and electron binding energy (EA) of the anion. The two most significant assumptions introduced into the model relate to how U^0 and L are designed to reflect the proper dependence on EA. Specifically, the L parameter is chosen to reproduce the known relationship between the radial size of the anion's orbital and the electron binding energy. The U^0 parameter is chosen so that the model's prediction of the electron binding energy (as $U^0-\varepsilon_i$) is the correct EA.

The non-BO couplings can be evaluated analytically within this model, and yield an electron detachment rate expression that offers insight into the electron ejection process. In particular, the crucial factors appearing multiplicatively in the integrals whose squares are proportional to the ejection rate are as follows:

(1) A factor $d\,\mathrm{EA}/dX[\mathrm{EA}+E]^{-1}$ that will be large if the separation between the anion and neutral energy surfaces (EA) is small and strongly varying ($d\,\mathrm{EA}/dX$ is large), and if the kinetic energy E carried away by the electron is small.
(2) A factor $[E/(E+U^0)]^{1/2}\{E+U^0\cos^2[E+U^0/\mathrm{EA}]\}^{-1/2}$ that (a) is small when E is small or when U^0 is large [recall $U^0=\mathrm{EA}(1+\pi^2/9)$] (b) is rather weakly dependent on E, otherwise, and (c) is also small at high E.

As noted earlier, these factors seem to agree with propensities that we have observed in our *ab initio* simulations of electron ejection rates.

In addition to the above propensities for transitions to occur near geometries where the anion and neutral surfaces approach closely and for which the ejected electron has neither very small nor very large kinetic energy, there are also vibrational energy and momentum propensities that contribute to the net rate.

Let us first consider the case in which the electronic $m_{i,f}$ matrix elements do not vary strongly with geometry. According to Eq. (38), this will occur when the anion and neutral energy surfaces have slope differences $(d\,\mathrm{EA}/dX)$ and spacings (EA) that are smoothly varying over the range of geometries accessed by the anion's vibrational motion. Such a situation would not arise, for example, for the cases shown in Fig. 2, where the $m_{i,f}$ elements are large in a narrow range of geometries, but could arise in the case illustrated in the right hand panel of Fig. 1.

In such cases, the geometry dependence of the $m_{i,f}$ can be factored out of the vibrational integral after which the latter reduces to an integral of the form

$$\langle \chi_f | d\chi_i/dX \rangle. \tag{39}$$

This integral can be treated as one does when computing Franck–Condon factors among vibrational states of two different electronic states, but with one modification. In the present case, as explained earlier, it is the derivative of one of the vibrational functions that occurs, because the electron ejection process requires that momentum (as well as energy) be transferred from the vibrational mode to the electron. So, the propensities arising in this case relate to the squares of the overlap of the anion's vibrational state lowered by one quantum level with the neutral molecule's vibrational functions χ_f. The anion's function is lowered by one quantum because $d\chi_i/dX$ generates, within the harmonic approximation, functions of one lower and one higher quantum number and only the former contributes to transfer of energy out of the vibrational mode.

The other limiting case to consider occurs when the $m_{i,f}$ elements are large over only a narrow range of molecular geometries (e.g., as in Fig. 2). In such a case, The integral $\int(m_{i,f}\chi_f\, d\chi_i/dX)dX$ ranges only over that region (e.g., $0<X<\delta$) where $m_{i,f}$ is significant. In this range, χ_i and χ_f oscillate with local de Broglie wave lengths of $h/(2\mu[\varepsilon_i - E^-(X)]^{1/2})$ and $h/(2\mu[\varepsilon_f - E^0(X)]^{1/2})$, respectively. Here, $E^-(X)$ is the anion's energy surface, $E^0(X)$ is the neutral's, μ is the reduced mass belonging to the vibrational mode, and ε_i and ε_f are the anion and neutral vibrational energies. Within the approximation where the $m_{i,f}$ elements are factored out of this integral (for this limited range of X), one can show that the integral will be small unless these two local de Broglie wavelengths are similar. In turn, this suggests that the local momenta $(2\mu[\varepsilon_i - E^-(X)])^{1/2}$ and $(2\mu[\varepsilon_f - E^0(X)])^{1/2}$ should be similar or that $\varepsilon_i - \varepsilon_f - E^-(X) + E^0(X)$ should be small. Notice that $\varepsilon_i - \varepsilon_f$ and

$[-E^-(X)+E^0(X)]$ are both positive quantities, so, once again, the propensities favor geometries where the anion and neutral surfaces are close and transitions for which $\varepsilon_i-\varepsilon_f=E$ is not large.

Although we find it gratifying that we now have analytical expressions for the E and EA dependencies of the non-BO-induced electron ejection rates, the fact is that the current experimental state of affairs does not yet permit a thorough testing of these predictions. Experiments in which anions are prepared in various known vibrational states and the rate of detachment of electrons into various vibrational levels of the neutral are what we need to test our model's predictions. On the other hand, the predictions offered by the model introduced here do agree with the results that we earlier obtained by carrying out state-to-state electron ejection rate calculations using *ab initio* quantum chemistry methods. This offers some evidence in favor of the validity, and thus the potential utility, of our analytical model.

ACKNOWLEDGMENTS

The support from NSF Grant No. 9982420 is gratefully acknowledged, and critical inputs from Professor Piotr Skurski and Professor Ken Jordan are much appreciated.

[1] The first paper we published on molecular anions dates to 1973: J. Simons and W. D. Smith, J. Chem. Phys. **58**, 4899 (1973); a few more recent overviews can be found in J. Simons, in *Photoionization and Photodetachment*, edited by C. Y. Ng (Advanced Series in Physical Chemistry, Vol. 10, Part II) (World Scientific, Singapore, 2000); J. Simons and P. Skurski, in *Theoretical Prospect of Negative Ions*, edited by J. Kalcher (Research Signpost, 2002), pp. 117–138; J. Simons and K. D. Jordan, Chem. Rev. **87**, 535 (1987).
[2] J. Simons, J. Am. Chem. Soc. **103**, 3971 (1981).
[3] P. K. Acharya, Rick A. Kendall, and J. Simons, J. Am. Chem. Soc. **106**, 3402 (1984).
[4] P. K. Acharya, R. Kendall, and J. Simons, J. Chem. Phys. **83**, 3888 (1985).
[5] G. Chalasinski, R. A. Kendall, H. Taylor, and J. Simons, J. Phys. Chem. **92**, 3086 (1988).
[6] D. O'Neal and J. Simons, J. Phys. Chem. **93**, 58 (1988).
[7] J. Simons, J. Chem. Phys. **91**, 6858 (1989).
[8] Our treatment of the dynamics of electron ejections was based on the pioneering work of R. S. Berry, who examined the mechanism of electron loss from highly electronically excited states of neutrals caused by vibration–rotation to electronic energy coupling: R. S. Berry, J. Chem. Phys. **45**, 1228 (1966).
[9] J. Simons, Adv. Quantum Chem. **35**, 283 (1999).
[10] J. Simons, J. Phys. Chem. A **102**, 6035 (1998).
[11] J. Simons, J. Phys. Chem. **103**, 9408 (1999).
[12] D. C. Clary, J. Phys. Chem. **92**, 3173 (1988); Phys. Rev. A **40**, 4392 (1989).
[13] We realize that it is an approximation to assume that the centrifugal potential can be treated as a single factor involving an average value of L^2 that does not vary as the molecule vibrates. In making it, we are assuming, for example, in the case illustrated on the left-hand side of Fig. 6, that the degree of s and of p orbital mixing in the σ-symmetry HOMO does not change as the molecule vibrates. This assumption is made when we take the form of the HOMO to be an angular function F, that does not depend on geometry, times a radial function as in Eq. (16). Although we do not believe making this assumption strongly affects the validity of our conclusions (except perhaps for very low E values where the centrifugal barrier will have its greatest effect), we intend to improve upon this aspect of the model in future work.